Studies of Catalyst-Controlled Regioselective Acetalization and Its Application to Single-Pot Synthesis of Differentially Protected Saccharides.

Sibin Wang,[†§] Oleksii Zhelavskyi,[†§] Jeonghyo Lee,[†§] Alonso J. Argüelles,[†] Yaroslav Khomutnyk,[†] Enoch Mensah,[†$] Hao Guo,[†] Rami Hourani,[†] Paul M. Zimmerman,[†*] and Pavel Nagorny.[†*]

[†]Chemistry Department, University of Michigan, 930 N. University Avenue, Ann Arbor, MI 48109

Chiral Phosphoric Acid, Acetalization, Regioselective, Protection, Carbohydrates, Computational Studies, Catalysis on Solid Support

ABSTRACT: This article describes the studies on regioselective acetal protection of monosaccharide-based diols using chiral phosphoric acids (CPAs) and their immobilized polymeric variants, (*R*)-Ad-TRIP-PS and (*S*)-SPINOL-PS as the catalysts. These catalyst-controlled regioselective acetalizations were found to proceed with high regioselectivities (up to >25:1 rr) on various *D*-glucose, *D*-galactose, *D*-mannose and *L*-fucose derived 1,2-diols, and could be carried in a regiodivergent fashion depending on the choice of the chiral catalyst. The polymeric catalysts were conveniently recycled and reused multiple times for gram scale functionalizations with catalytic loading as low as 0.1 mol%, and their performance was often found to be superior to the performance of their monomeric variants. These regioselective CPA-catalyzed acetalizations were successfully combined with common hydroxyl group functionalizations as single-pot telescoped procedures to produce 34 regioisomerically pure differentially protected mono- and disaccharide derivatives. To further demonstrate the utility of the polymeric catalysts, the same batch of (*R*)-Ad-TRIP-PS catalyst was recycled and reused to accomplish single-pot gram-scale syntheses of 6 differentially protected *D*-glucose derivatives. The subsequent exploration of the reaction mechanism using NMR studies of deuterated and nondeuterated substrates revealed that low-temperature acetalizations happen via *syn*-addition mechanism, and that the reaction regioselectivity exhibits strong dependence on the temperature. The computational studies indicate complex temperature-dependent interplay of two reaction mechanisms, one involving an anomeric phosphate intermediate and another via concerted asynchronous formation of acetal that results in *syn*-addition products. The computational models also explain the steric factors responsible for the observed C2-selectivities and are consistent with experimentally observed selectivity trends.

1. INTRODUCTION

Carbohydrates are essential molecules that not only serve as immediate energy sources, but are also associated with numerous biological activities. Accordingly, the studies of carbohydrates have been the focus of many ongoing investigation in the fields of organic chemistry, biochemistry, and drug discovery.[1] However, in many instances, gaining access to complex oligosaccharides and glycoconjugates has been the bottleneck for the exploration of their biological and medicinal properties.[2] Complex oligosaccharides are comprised of the simpler monosaccharides, and, not surprisingly, modern synthetic approaches to oligosaccharides strongly rely on the ability to access differentially protected building blocks. Synthesis of such differentially protected monosaccharides often requires multiple step sequences to differentiate numerous hydroxyl groups, and may suffer from low yields and tedious purifications due to the formation of undesirable regioisomers throughout these sequences.[3] To address the challenges associated with the selective functionalization of monosaccharides, numerous methods, including single pot functionalization approach by the Hung group, have been previously developed.[4,5] However, the majority of such methods rely on the reagents and catalysts that discriminate between the axial and equatorial hydroxyl groups while only few methods exist for the selective differentiation of equatorial hydroxyl groups that are in similar steric and electronic environment (*cf.* Scheme 1A).[6,7] While possible with achiral reagents or catalysts, such transformations often exhibit strong electrophile- and substrate structure dependence and lack generality (*cf.* Scheme SI-1 for compiled representative examples). Pioneered by the Miller group,[8] the approaches based on the use of asymmetric catalysts to achieve site-selective functionalization of sugar-derived polyols have recently gained significant attention.[8-11] While many efforts, most notoriously by the Kawabata,[9] and Tang[10] groups have focused on exploring asymmetric catalysts for the selective acylation reactions, chiral catalyst-controlled site-selective phosphorylation, thiocarbonylation, sulfonation, silylation, acetalization and glycosylation have also been explored in the context of chiral catalyst-controlled functionalization of sugar-derived polyols.[11]

We have long-standing interests in utilizing chiral phosphoric acids as the catalysts leading to regio- and stereoselective acetal formation.[12-14] As the part of these studies our group

disclosed selective functionalization of monosaccharides using 1,1'-bi-2-naphthol (BINOL)-derived chiral phosphoric acids (CPAs)[15] as the catalysts to direct regioselective acetalization of carbohydrate-derived 2,3-diols (*cf.* Scheme 1B).[13] This study demonstrated that (*R*)-CPA catalyst **1** could promote regioselective protection of *D*-glucose, *D*-galactose, *D*-mannose-derived diols and a *L*-fucose-derived triol with enol ethers such as dihydropyrane (DHP), 2-methoxypropene (2-MP), and 1-methoxycyclohexene (1-MCH). The reactions of *D*-glucose and *D*-galactose derivatives proceeded at the sites that cannot be directly functionalized with achiral reagent such as *n*-dibutyltin(IV) oxide (*cf.* Scheme SI-1).[6d] In addition, it was observed that the chirality of the catalyst played an important role as using the (*S*)-**1** or achiral acids such $(PhO)_2PO_2H$ resulted in unselective reactions or selectivity switch. Importantly, these transformations featured mild reaction conditions and the use of easily available and non-toxic substrates and catalysts.

Scheme 1. Synthetic challenges and summary

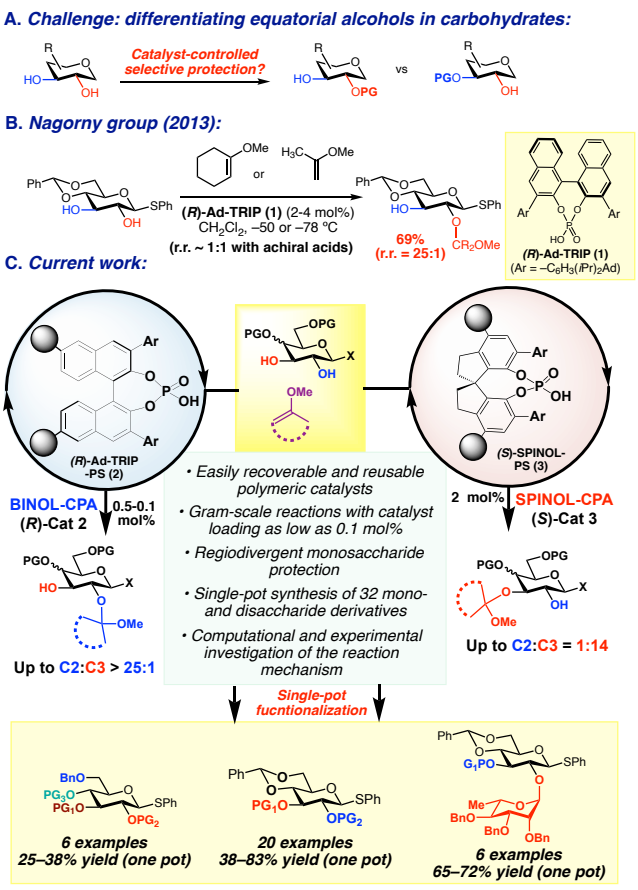

Building on this approach, the current article expands the substrate scope and demonstrates the use of CPA-catalyzed regioselective acetalizations for the scalable single-pot synthesis[16] of various differentially protected *D*-glucose, *D*-galactose and *D*-mannose mono- and disaccharides (Scheme 1C). These telescoped single-pot multiple step protocols proceed with high selectivities and efficiencies and require minimum purifications to access valuable protected building blocks from commercially available diol precursors. To address the challenges associated with the accessibility of the catalyst **1**, we describe the development of immobilized catalysts **2** and **3** that was found to promote highly selective acetalization reactions and could be recycled and re-used multiple times. The use of catalyst **2** that is structurally equivalent to **1** allowed to achieve substantial reduction of the catalyst loading (0.5 to 0.1 mol% for gram-scale reactions) and significantly improve the selectivity of acetalization for several different substrates. In addition, catalyst **3** allowed regiodivergent protection at positions that cannot be accessed using catalysts **1** or **2**.

Scheme 2. Site-selective MOC and MOP protection of monosaccharide-derived diols[a]

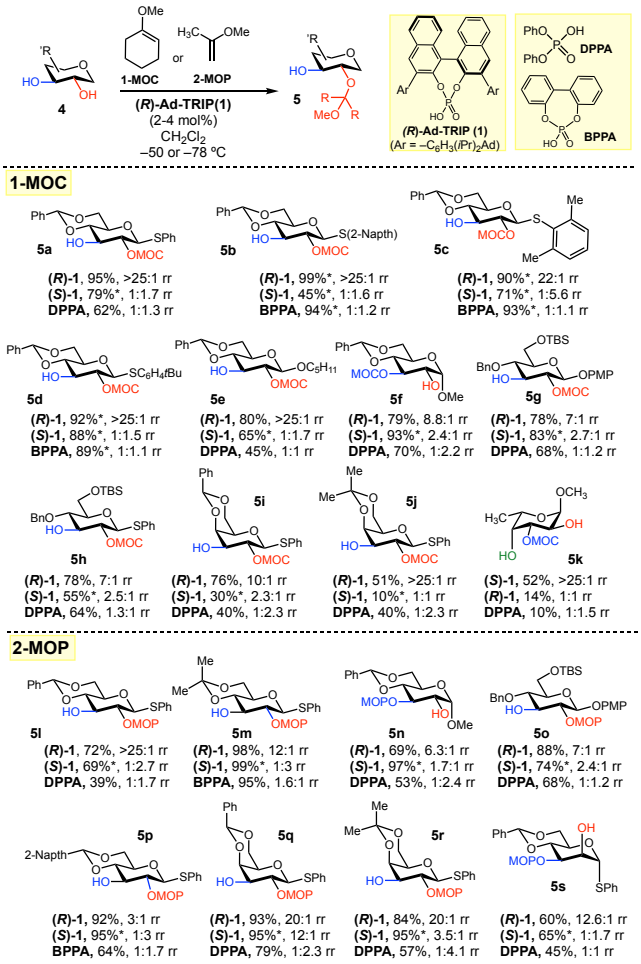

[a]The reactions with 2-methoxypropene (2-MOP) were performed overnight at –78 ºC and the reactions with 1-methoxycyclohexene (1-MOC) were performed overnight at –50 ºC on 0.056 mmol scale (0.042 M solution) for 18-24 h in the presence of 4Å MS. The reaction with **4a** was performed on 2.78 mmol (1.0 g) scale. These rr values were determined by ^{1}H

NMR analysis of the crude reaction mixtures of the products **5** and **6** as well as their acetylated derivatives. The values with asterisk* represent conversion determined by ^{1}H NMR analysis, and each entry represents an average of 2 experiments.

Finally, this article summarizes the mechanistic and computational QM/MM studies of the acetalization reaction mechanism and reveals that this transformation may proceed through an interplay of two different reaction mechanisms with the asynchronous concerted acetalization mechanism being dominant at low temperatures and leading to the observed selective formation of acetals. These insights into the reaction mechanism were used to develop a stereochemical model explaining the observed selectivity trends.

2. DISCUSSION

Selective protection of a single alcohol moiety as an acetal within a sugar-derived diol possessing alcohols in similar steric and electronic environment represents a challenge. Acid-catalyzed acetal formation is known to proceed through the highly reactive intermediates– oxocarbenium ions, which are known to react with nucleophiles indiscriminately. The resultant acetals are also acid labile, and equilibration/isomerization leading to the most thermodynamically stable product under the reaction conditions is not uncommon. Being very useful in organic synthesis and carbohydrate chemistry, mixed acetal protecting groups such as 1-methoxycyclohexyl (MOC) and 2-methoxy-2-propyl (MOP) are very sensitive to acids and may easily hydrolyze and/or undergo the formation of 1,3-dioxolanes and 1,3-dioxanes.[17]

With these considerations in mind, it was particularly surprising to observe that **(*R*)-Ad-TRIP** (**1**)-catalyzed formations of MOC and MOP acetals often proceeded with great levels of regiocontrol and high yields (*cf.* Scheme 2 and SI Scheme 2S).[13,14] Remarkably, the control experiments with various achiral phosphoric acids such as DPPA and BPPA as well as *p*-TSA and CSA did not lead to selective reactions, and approximately equimolar mixtures of the C2 and C3 protected acetals were obtained in each instance in diminished yields. Similarly, the use of enantiomeric **(*S*)-Ad-TRIP** catalyst **1** often resulted in diminished yields and selectivities, and in the instance of **5c**, **5l**, **5m**, and **5p** the selectivity was reversed to produce significant amounts of the C3-regioisomer. Not surprisingly, the use of *L*- rather than *D*-sugars such as *L*-fucose-derived triol **4k** required **(*S*)-** rather than **(*R*)-1** to achieve selective protection of the C3 position.

Scheme 3. Regioselective single-pot synthesis of the differentially protected mono- and disaccharide derivatives enabled by (*R*)-Ad-TRIP(1)-catalyzed regioselective MOC- and MOP-protections[a]

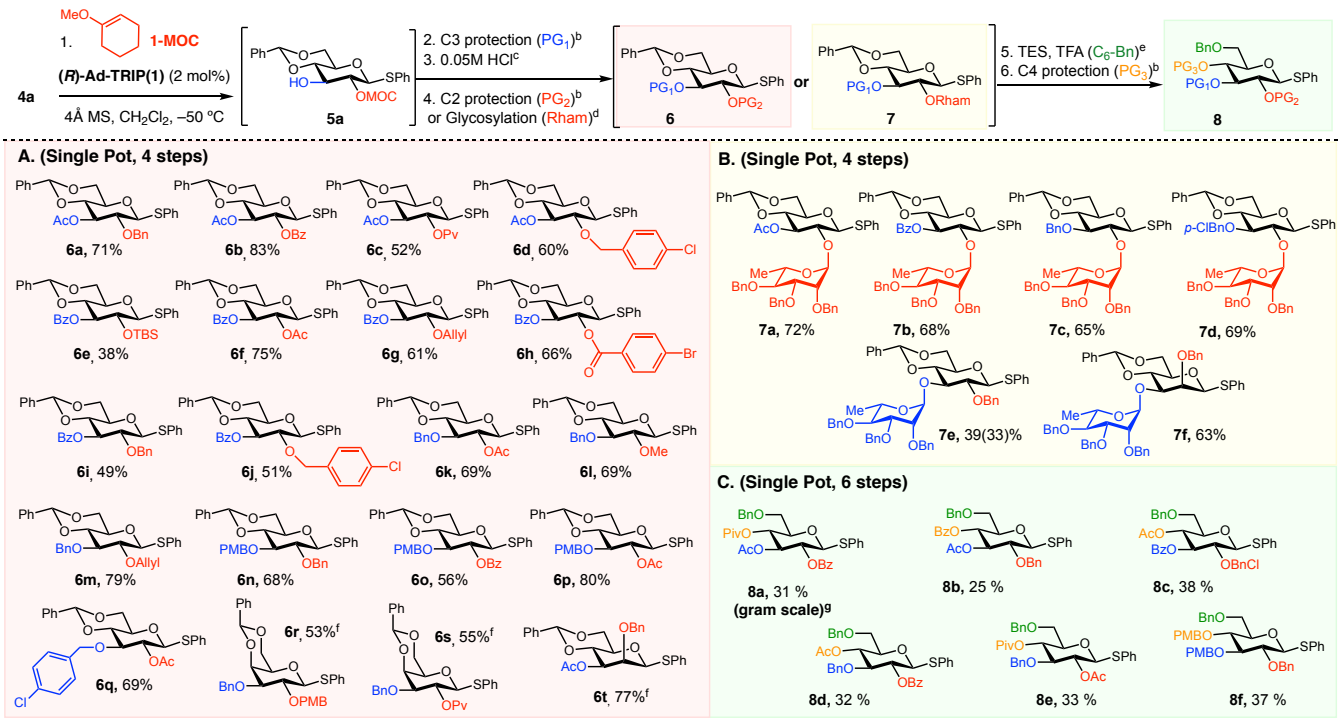

[a]Isolated yield after one-pot sequence leading to **6**. The reaction mixtures were concentrated by the stream of N_2 prior to each protection step. Unless noted otherwise, these experiments were carried on 0.056 mmol scale. MOC protection was accomplished as described in Scheme 2. [b]Acylations were carried using Ac_2O (1.1 equiv), DMAP (10 mol%), Et_3N (5.0 equiv) or BzCl (1.2 equiv), DMAP

(20 mol%), Py (10 equiv). Alkylation was accomplished by addition of NaH (1.2 equiv), alkyl halide (1.1 equiv), TBAI (0.1 equiv) and DMF (cat). [c]The MOC cleavage was achieved by addition of 0.05M HCl in CH_2Cl_2 (pH=5). [d]The final glycosylation step to form **7a** and **7b** was accomplished with 2.5 equiv of and TMSOTf (20 mol%) in DCM at 0 ºC in the presence of 4 Å MS. The glycosylations leading to **7c-7f** was accomplished in the presence of 1.4 equiv of *tris*-benzylated *L*-rhamnose trichloroacetimidate. [e]Compounds **6r-6t** were generated using MOP-protected intermediates **5q** and **5s**. [f]Benzylidene acetal cleavage was accomplished using Et_3SiH (5 equiv), CF_3CO_2H (5 equiv), DCM, 0 ºC, 2h. [g]The synthesis of **8a** was carried on 1.0 g scale. Please refer to SI for the detailed description of these single-pot protocols.

The *D*-glucose derivatives possessing 4,6-benzylidene acetal protection and featuring β-configuration at the anomeric position exhibited highest levels of regiocontrol exclusively providing the C2-protected products **5a–5e** and **5l**. The size and nature of the anomeric substituent with β-configuration seemed to have little effect on the reaction selectivity; however, the changes in the 4,6-acetal moiety seemed to have a significant effect. Thus, the **(*R*)-1**-catalyzed 2-MOP protection leading to 2-naphthyl product **5p** proceed with the significantly lower C2-selectivity (3:1 rr) then for the corresponding benzylidene acetal derivative **5l** (>25:1 rr). In line with this observation, the analogous to **5l** acetonide derivative **5m** was produced in only 12:1 rr while the MOP-derivative **5o**. Similarly, MOC protection leading to the derivatives **5g** and **5h** lacking the 4,6-benzylidene acetal moiety were produced with lower C2 selectivities (5:1 and 7:1 rr, correspondingly) then for the benzylidene acetal containing products **5a-5e**. Finally, it should be noted that the presence of the axial substitution next to the C2/C3 diol seems to direct the protection to the position furthest away from the axial substitution. Thus, both the MOC and 2-MOP protection of *D*-galactose derivatives with β-anomeric configuration, **4i** and **4j**, provided C2-protected products **5i**, **5j**, **5q** and **5r** in good-to-excellent selectivities and yields. Following this trend, *D*-glucose derivative with α-methoxy configuration **4f** provided the C3 (rather than the C2) products **5f** and **5n** in moderately good selectivities (8.8:1 rr and 6.3:1 rr, correspondingly).

While mixed acetal protecting groups are less common in carbohydrate synthesis than acyl or benzyl protection, their stability to bases and significant lability under the mildly acidic conditions offer excellent opportunities for carrying out the subsequent functionalizations in a single operation. Therefore, our following studies were focused on demonstrating that regioselective products **5a-5s** are of great utility for the telescoped preparation of differentially protected monosaccharide derivatives from commercially available building blocks such as **4a**. Inspired by the streamline method for the single-pot synthesis of various *D*-glucose derivatives by the Hung and coworkers,[4] we investigated one-pot derivatizations of **5a** (*cf.* Scheme 3). Considering that both the MOC and 2-MOP protecting groups are highly labile in the presence of an acid (*vide supra*), our single pot protocol included *in situ* removal of the MOC protection with 0.05 M HCl without deprotecting the 4,6-benzylidine acetal.[17] The high volatility of 0.05 M HCl solution in DCM was also suitable for the overall single-pot functionalization process as it could be removed by passing a nitrogen stream over the reaction mixture without the necessity of carrying the reaction work up.

The one-pot transformations leading to differentially protected C2/C3 products **6a-6t** (*cf.* Scheme 3A) commenced with CPA (**1**)-directed regioselective acetalization, and the resultant C2-acetal **5a** (or **5q** and **5s**) was successfully obtained in full conversion. At this point, the mixture was dried by sequentially applying a gentle N_2 flow and flask evacuation before the next step. Initially the crude mixture containing compound **5a** was subjected to free C3-hydroxyl group protection without affecting the C2-acetal. Since mixed acetals are acid- and heat- labile, acidic conditions and high reaction temperatures were avoided. The regioselective acylations of the C3-OH were accomplished using $(RCO)_2O$/Py or RCOCl/Et_3N in the presence of catalytic DMAP (substrates **6a–6j**). Alternatively, the C3-alkylation was accomplished using alkyl halides and sodium hydride as the base in the presence of catalytic TBAI (**6k–6t**). The C2 MOC (or MOP) acetal was removed by adding excess of HCl solution in DCM to the reaction mixture. The resultant acidic solutions were concentrated by passing N_2 stream to blow out the volatiles and subsequent evacuation of the reaction vessel, and the concentrated crude oils were subjected to the C2-protection to provide products **6a-6t** in good yields (49-83% overall yield). In addition to the *D*-glucose-based derivatives **6a-6q**, this method was also successfully applied to generate *D*-galactose-based substrates **6r** and **6s** as well as *D*-mannose-derived substrate **6t** using MOP (rather than MOC) protection strategy. Unlike other substrates, *D*-mannose derivative **5s** contained MOP acetal at the C3 position, which required functionalization in a reverse way (C2-benzylation, C3-acetal cleavage, and C3-acetylation) to afford compound **6t** in good overall yield (77%) and selectivity (>12:1 rr for the first step).

It is noteworthy that while some of the derivatives (i.e. **6k–6q**) might be potentially accessible through one-pot glucose functionalization strategy developed by the Hung group, one-pot synthesis of the derivatives **6a–6j** featuring the C3 acyl protection has not been previously described and would be challenging to accomplish via Hung's single-pot protocol in good yields. Similarly, previously published one-pot protection protocols could not be readily adopted to the synthesis of *D*-galactose and *D*-mannose derivatives similar to **6r–6t**. Finally, the operational simplicity for the deprotection of the MOC and MOP groups allows to expand the scope of the protecting groups (to include substrates

like **6e**) and achieve flexibility in controlling the C2/C3 protection to generate regioisomeric substrates like **6d** and **6q** in similar yields (60% and 69%, correspondingly).

The aforementioned regioselective manipulations on **4a** could be combined with glycosylation to accomplish concomitant protection and glycosylation of the C2 and C3 positions (*cf.* Scheme 3B). Thus, CPA-catalyzed C2-protection with MOC was followed with acylation (**7a** and **7b**) or alkylation (**7c** or **7d**), subsequent MOC group cleavage, and glycosylation with 2,3,4-OBn *L*-rhamnopyranoside trichloroacetimidate to provide derivatives **7a-7d** in good yields (65-72%) as single regioisomers with the glycosylated C2 position. This protocol was also extended to other sugars such as *D*-mannose (**4s**) to provide the protected and glycosylated derivative **7f** as the single regioisomer in 63% yield. The inclusion of the additional C2 protection/C3 deprotection sequence also allowed to achieve the reverse glycosylation of the C3 position and resulted in the derivative **7e** in moderate yield (39%). Importantly, the C3 hydroxyl group in **4a** is more reactive in glycosylation with 2,3,4-OBn *L*-rhamnopyranoside trichloroacetimidate, and the direct glycosylation of **4a** provides ~3:1 mixture of the regioisomeric C3 and C2 products in 79% overall yield. Correspondingly, the described strategy offers advantages for the synthesis of C2 glycosides such as **7a–7d**.

These transformations could be further combined with benzylidene acetal opening/C4 protection steps to accomplish single-pot generation of differentially protected *D*-glucose derivatives **8a–8f** depicted in Scheme 3B. Thus, the previously developed protocol included regioselective benzylidene acetal reduction with CF_3CO_2H/Et_3SiH leading to product containing free C4 alcohol that was subsequently protected. These single-pot transformations proceeded in 25-38% overall yield (~85% yield per operation) with high levels of overall regiocontrol. These procedures were scalable, and the derivative **8a** was made on 1.0 g scale (31% yield) with the same yield as on 0.056 mmol scale.

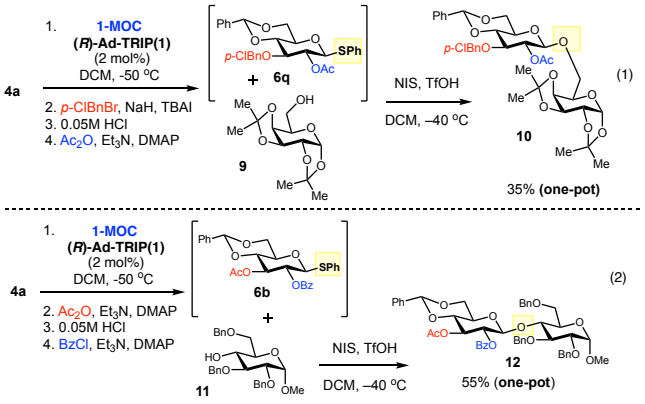

The substrates **6a–6t** carry a thiophenol moiety at the anomeric position, and, hence, could serve as glycosyl donors (Eq. 1 and 2). Thus, we selected two derivatives of **4a** (i.e. **6b** and **6q**) and demonstrated that the regioselective protection leading to **6b** and **6q** could be combined with glycosylation using acceptors **9** and **11** and leading to single pot formation of disaccharides **10** and **12**. While the yield of **10** (35%) was diminished due to the lability of acetonide moieties in **9** and **10** under the acidic conditions (Eq. 1), the single pot synthesis of **12** proceeded in good yield (55%) and selectivity (Eq. 2).

We believe that the aforementioned results demonstrate that CPA-catalyzed regioselective acetalizations are of great use for the single pot protection and glycosylation of monosaccharides. While this method allows to expand the repertoire of sugar derivatives and transformations developed by Hung, it suffers from the obligatory use of expensive chiral acid **(*R*)-Ad-TRIP** (**2**). We surmised that the costs associated with the use of **2** could be dramatically reduced if the catalyst is immobilized on a solid support as numerous recent studies suggest that such catalysts could be readily recovered and recycled or employed for the catalysis in continuous flow.[18]

Scheme 4. Synthesis and applications of polystyrene-supported CPA catalyst (*R*)-Ad-TRIP-PS (2) and (*S*)-SPINOL-PS (3)

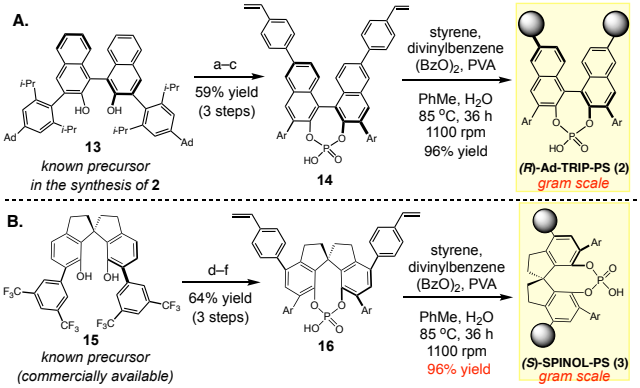

C.

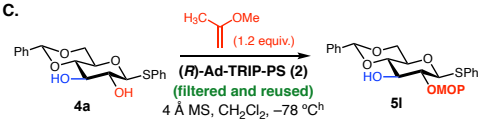

cycle number	CPA loading (mol%)	scale	time	conversion (%)	C2:C3 (r.r.)
1	0.5	1.0 g	18 h	99	>25:1
2	0.5	1.0 g	18 h	95	23:1
3	0.5	1.0 g	18 h	97	>25:1
4	0.5	1.0 g	18 h	99	>25:1
5	0.5	1.0 g	18 h	97	>25:1
6	0.5	1.0 g	18 h	99	>25:1
7	0.5	1.0 g	18 h	99	>25:1
8	0.5	1.0 g	18 h	99	>25:1
9	0.5	1.0 g	18 h	99	>25:1
10	**0.1**	**5.0 g**	**36 h**	**99**	**>25:1**

(a) **13** (1 equiv), Br_2 (2.2 equiv), DCM (0.16 M), –78 ˚C, 2.5 h, 92%; (b) 4-vinylphenylboronic acid (2.4 equiv), K_2CO_3 (4.0 equiv), EtOH:THF = 1:1 (0.1 M), $Pd(PPh_3)_4$ (15 mol%), reflux, 12h, 65%; (c) $POCl_3$ (2.0 equiv), pyridine (0.1 M), 70 ˚C, 12 h, then H_2O (0.1 M) 100 ˚C, 16 h, 57%; (d) **15** (1 equiv), Br_2 (2.2 equiv), DCM (0.16 M), –78 ˚C, 2.5 h, 97%; (e) 4-vinylphenylboronic acid (5 equiv), K_2CO_3 (5.0 equiv), dioxane:water=2:1 ratio (0.066 M), $Pd(PPh_3)_4$ (5 mol%), 70 ˚C, 5h, 88% yield; (f) $POCl_3$ (5.0 equiv), pyridine (0.1 M), 70 ˚C, 12 h, then H_2O (0.1 M) 100 ˚C, 16h, 75%.

Therefore, our subsequent efforts were focused on developing a catalytically active immobilized version of **1** (cf. Scheme 4 and SI Scheme 3).[19] Based on the previously developed strategies for TRIP immobilization,[20a] we investigated this variant for the synthesis of immobilized on polystyrene support catalyst **(*R*)-Ad-TRIP-PS (2)**. While the previously published route did not lead to catalytically active in acetalization reactions **(*R*)-Ad-TRIP-PS (2)**, we were able to modify this approach (cf. Scheme 4A) to produce a viable immobilized catalyst **2**. Based on our previous observation that (*S*)-SPINOL CPA derived from **15** may lead to regiodivergent acetalization, we also pursued preparation of new immobilized (*S*)-SPINOL-PS (**3**)[20b] depicted in Scheme 4B, using the approach developed for the synthesis of **2**. Remarkably, the gram scale syntheses of **3** was accomplished in only 4 steps from **15** that is a commercially available derivative of (*S*)-SPINOL. Gratifyingly, both immobilized catalysts **(*R*)-Ad-TRIP-PS (2)** and **(*S*)-SPINOL-PS (3)** were found to efficiently promote the catalytic activity and selectivity in acetalization of **4a** and could be conveniently recovered and recycled by filtration and

Scheme 5. Regiodivergent protection of monosaccharides with immobilized catalysts (*R*)-Ad-TRIP-PS (2) and (*S*)-SPINOL-PS (3), and the use of recycled (*R*)-Ad-TRIP-PS (2) for multiple gram-scale regioselective syntheses of differentially protected *D*-glucose derivatives 6a, 6f, 6k, 6p, and 8e.

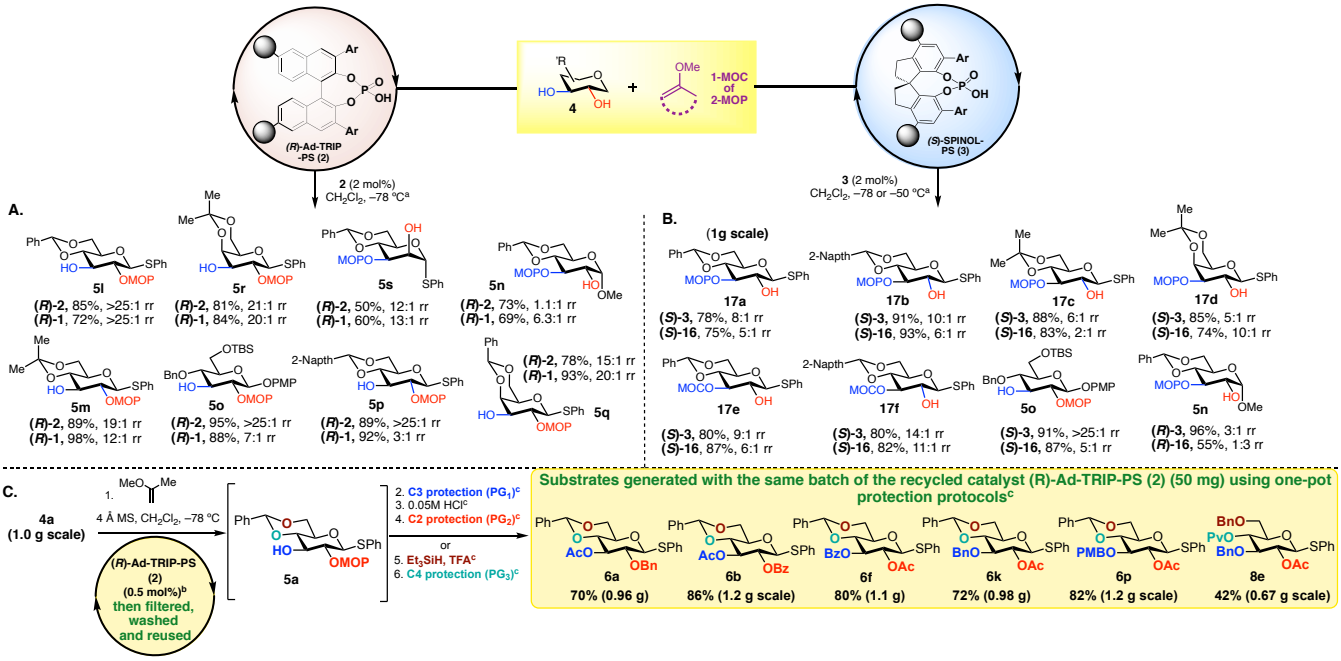

[a]The reactions were performed with 2 mol% of catalysts **1–3** or **16** at either –78 ºC (2-MOP-protection) or at –50 ºC (1-MOC-protection) on 0.056 mmol scale (1.0 g, 3 mmol scale for substrate **17a**) as 0.042 M solutions in DCM for 18-24 h in the presence of 4Å MS. The rr values were determined by ^{1}H NMR analysis of the crude reaction mixtures of the products **5** and **17** as well as their acetylated derivatives. Each entry represents an average of 2 experiments. [b]These experiments were performed with 50 mg (0.5 mol%) of catalyst **2** as described in Scheme 4. The reaction mixture was quenched with Et_3N and the catalyst **2** was filtered, washed and reused as described in Scheme 4 and SI Section XVI. [c]The single pot-protection for steps 2-4 was executed following the protocols described in Scheme 3 and Scheme SI-Y. The yields represent the yield for the overall single operation from **4a**.

wash (*cf.* Scheme 4C, and Tables SI-1S and SI-2S). Most importantly, we were able to repeatedly run nine consecutive 1.0 g scale MOP-protections of **4a** with only 0.5 mol% (50 mg) of the same batch of catalyst **2** without erosion in yield or selectivity. Then, using the same batch (i.e. 0.1 mol% loading) of **2**, a 5.0 g scale acetalization gave **5a** in >25:1 rr, and 99% conversion. These results indicate that significant catalyst economy was achieved as the same 50 mg of **2** were used to convert the total of 14.0 g of **4a** into **5a**. Importantly, parallel evaluation of catalyst **1** at 0.5 mol% loadings indicated that such reactions were also possible; however, it

was required twice as much time as for **2** (i.e. 36 h vs 18 h) to achieve full conversion.

Based on the these promising results for the regioselective acetalization of **4a** using immobilized catalysts **2** and **3**, our subsequent studies focused on investigating these polymeric catalysts in the acetalizations of other substrates and comparing them to the monomeric catalysts **1** and **16** (*cf.* Scheme 5A and 5B). Gratifyingly, (*R*)-Ad-TRIP-PS catalyst **2** demonstrated a great selectivity profile for the generation of the corresponding 2-MOP protected derivatives, and with the exception of one case (**5n**), the resultant products were obtained in excellent C2-selectivity (*cf.* Scheme 5A). It is noteworthy that the selectivities and yields for substrates **5l**, **5r**, and **5s** obtained with the immobilized catalyst **2** matched the corresponding results previously obtained for CPA **1**. Remarkably, in three instances (**5m**, **5o**, and **5p**), PS-supported CPA **2** provided significantly higher regioselectivities then the monomeric acid **1** (25:1 rr vs 3:1 rr for **5p**, 25:1 rr vs. 6:1 rr for **5o**, and 19:1 rr vs 12:1 rr for **5m**). Finally, in instances of **5n** and **5q**, the selectivities obtained with **2** were lower than the selectivities obtained with **1** (1:1 rr vs 6:1 rr for **5n** and 20:1 rr vs 15:1 rr for **5q**).

The subsequent evaluation of (*S*)-SPINOL-PS catalyst (**3**) resulted in regiodivergent acetalization of substrates **4a**, **4j**, **4m**, and **4p**, leading to the regioisomeric C3 acetals **17a–17f** in good to excellent selectivities; however, in the case of substrates **4f** and **4h**, the same regioisomers as with (*R*)-Ad-TRIP (**1**) and (*R*)-Ad-TRIP-PS (**2**) were observed. The selectivities improved with increasing steric size of the O4/O6 acetal (from 6:1 to 8:1 to 10:1 rr for **17c**, **17a**, and **17b**). Similarly, increasing the steric size of electrophile (i.e. 1-MOC vs. 2-MOP) consistently resulted in an improvement of the reaction selectivities (from 10:1 for **17b** to 14:1 for **17f** and from 8:1 for **17a** to 9:1 for **17e**). To demonstrate the scalability of the process, the synthesis of **17a** with **(*S*)-3** was successfully carried on 1.0 g (2.78 mmol) scale with improved 94% yield and 8:1 rr.

It is noteworthy that as in the case of the (*R*)-Ad-TRIP-PS (**2**), the use of (*S*)-SPINOL-PS(**3**) may lead to significant improvement in the reaction selectivity in comparison to the monomeric catalyst **16**. Such improvements in selectivity were observed for substrates **17a–17c**, **17e**, **17f** and **5o** although for **17d** polymeric catalyst was inferior to **16**. Remarkably, complete switch in selectivity was observed in the case of substrate **4f**, and while polymeric **(*S*)-3** resulted in moderately selective formation of the C3-protected product **5n** (3:1 rr), monomeric **(*S*)-16** resulted in the formation of the C2 regioisomer of **5n** (1:3 rr). These observations suggest that the additional structural features present in **2** and **3** that are not present in **1** and **16** such as the linker and polystyrene matrix may impact the steric interactions between the CPA and substrate. This could have both positive or negative consequences for the reaction outcome although in the majority of cases presented in Schemes 5A and 5B improvements in the selectivity were observed.

Scheme 6. A. Selectivity versus temperature profile for the MOC and 2-MOP protection of 4a, and theoretically predicted selectivity profile for a reaction with no mechanism switch using Arrhenius model with ΔΔG‡ = 1.2 kcal/mol.[a] B. Control equilibration experiment.[b] C. Potential reaction mechanisms for the CPA-catalyzed acetalization reaction.

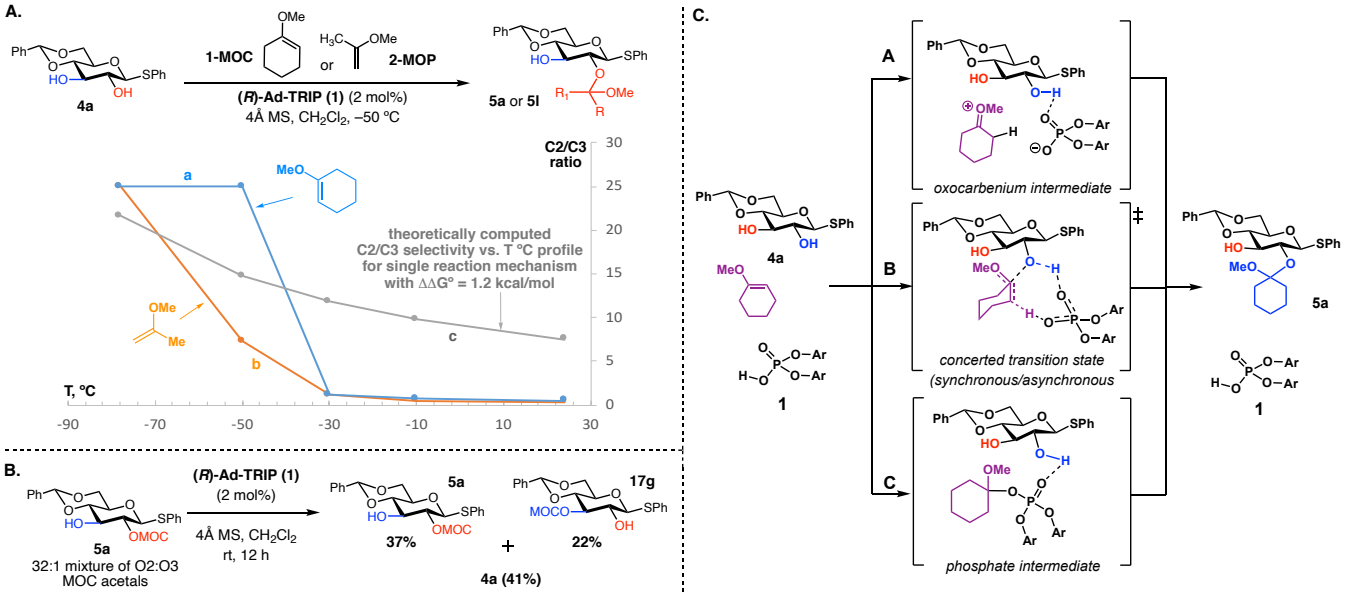

[a]The reactions with 2-methoxy-2-propene (2-MOP) and 1-methoxy-1-cyclohexene (1-MOC) were performed overnight at the specified temperature on 0.056 mmol scale (0.042 M solution) in the presence of 4Å MS. The C2/C3 ratio was determined by ^{1}H NMR

analysis of the crude mixture. [b]Compound **5a** containing 32:1 mixture of C2:C3 MOC acetal regioisomers was subjected to the standard acetalization conditions above without 1-MOC at r.t. for 12 h. The resultant mixture composition was analyzed by ^{1}H NMR.

To demonstrate the utility of the immobilized CPAs for the gram scale synthesis of differentially protected monosaccharide derivatives, we performed series of 1.0 g scale functionalizations of **4a** using the same batch (50 mg or 0.5 mol%) of (*R*)-Ad-TRIP-PS **3** (*cf.* Scheme 5C). The selective MOP-protections of **4a** were followed by filtration, and the filtrate was subjected to the previously developed one-pot derivatizations (*cf.* Scheme 3). The recovered and recycled catalyst **3** was then reused to accomplish subsequent cycles of regioselective functionalization of **4a**. This protocol allowed consecutive one-pot syntheses of **6a** (0.96 g), **6b** (1.2 g), **6f** (1.1 g), **6k** (0.98 g), **6p** (1.2 g), and **8e** (0.67 g) using the same batch of catalyst **3** (50 mg). It is also noteworthy that the single-pot procedures leading to **6a**, **6b**, **6f**, **6k**, **6p**, and **8e** were readily scalable and proceeded with improved overall yields. Altogether, these studies suggest that immobilized CPA-catalysts **2** and **3** hold great potential for the regioselective preparation of differentially protected monosaccharide derivatives, and that the use of the regioselective CPA-catalyzed acetalization allows the expansion of the single-pot methods previously developed by Hung and others.[4,5]

With these developments in hand, our subsequent studies were focused on experimental and computational exploration of the mechanism for the regioselective acetalizations and development of a stereochemical model explaining the observed selectivity trends. Both MOC and MOP acetalizations demonstrated unusual selectivity versus temperature profiles (*cf.* Scheme 6A). Thus, both types of acetalization were unselective at the temperatures above –30 ºC, but demonstrated significant jump in selectivity once cooled below –50 ºC. These unusual temperature vs. selectivity profiles are not consistent with the theoretically predicted using Arrhenius model regioselectivity on temperature dependence computed for $\Delta\Delta G^{º}$=1.2 kcal/mol (*cf.* Scheme 6A and SI Figure 2S). The regioselectivity should be exponentially dependent on temperature, and the profiles in Scheme 6A should not involve abrupt increase of selectivity at some threshold temperature. The observed temperature dependence suggests that the acetalization may happen through competing mechanisms, and that the mechanism prevailing at the temperatures below –50 ºC might be different from the reaction mechanism at higher temperatures. To test whether the product is stable at higher temperatures, regioisomerically enriched product **5a** was re-subjected to acid **1** at room temperature (Scheme 6B) for 12 h. This resulted in significant isomerization of **5a** into the regioisomeric product **17g**, and the crude reaction mixture contained ~1.7:1 ratio of **5a**:**17g**. The significant amounts of diol **4a** were also present in the mixture and suggested that the formation of **17g** proceeded through **4a** and that the overall acetal formation is reversible at room temperature.

With these observations in mind, three different reaction mechanisms depicted in Scheme 6C were proposed. These involved the conventional mechanism proceeding through the oxocarbenium ion (option A),[21] as well as direct synchronous or asynchronous concerted addition, as previously proposed by us for CPA-catalyzed spiroketalizations (option B).[12c] Alternatively, the catalyst may react with the MOC or 2-MOP enol ethers to form a phosphate intermediate, which then proceeds through S_N1 or S_Ni mechanisms that were observed by us for CPA-catalyzed glycosylation of 6-dEB (option C).[12b,22] Differentiating these mechanistic options computationally represents a challenging task as it requires finding and optimizing conformationally flexible transition states structures. To address some of these challenges, our computational studies used the reaction-path and transition-state search tool called the Growing String Method (GSM).[23,24] The large size of the system (207 atoms) motivated a Quantum Mechanics/Molecular Mechanics (QM/MM) approach to make the reaction path analysis feasible. The QM/MM borders were set on the C-C bond at the 3,3'-positions of the chiral catalyst ***(R)*-2** placing bulky hydrocarbon moieties in the MM region (*cf.* Scheme **7S - SI**).

Reaction pathways were determined using GSM for the 20 lowest energy conformers for each path (C2 and C3 in each mechanism, *cf.* SI). The concerted mechanism was investigated first, beginning from the complex involving the substrate H-bonded to **(*R*)-2** (Figure 1A). The reaction pathway shows an asynchronous concerted transformation: the CPA protonates the enol ether (PG) to generate an oxocarbenium cation that then reacts with the OH-group of the sugar substrate **4a** (TS_1 for C2-path and TS_2 for C3-path). The resultant CPA anion deprotonates the OH-group synchronously with oxygen nucleophilic attack on the oxocarbenium cation. The lowest energy activation barriers among the 20 conformers of each TS favour C2-protected product **5a** formation at 223K ($\Delta\Delta G^{‡}_{223}$ = –1.2 kcal/mol) and 273K ($\Delta\Delta G^{‡}_{273}$ = –1.0 kcal/mol) (Table 6S-SI). Activation energies ($\Delta G^{‡}$, kcal/mol) for this mechanism (21.1 and 22.3 kcal/mol for C2- and C3-pathways respectively) are slightly higher than expected from the experimental data (18-19 kcal/mol for overnight reaction at –50 °C). This concerted mechanism, which does not show an oxocarbenium intermediate (Scheme 6C, Path A), does bear similarities with the oxocarbenium mechanism. In particular, the oxocarbenium ion appears along the reaction path at the transition state structure, which identifies the concerted mechanism as asynchronous (Scheme 6C, Path B).

The two-elementary-step phosphate-mediated mechanism (Scheme 6C, Path C) was investigated next. To do so, 20 conformationally distinct reaction pathways involving **(*R*)-(2)** and 1-methoxycyclohexene (**PG**) were examined. The phosphate intermediate is reached via asynchronous protonation of the enol ether **PG** followed by nucleophilic

attack with the same phosphoric acid oxygen that participated in substrate protonation. The activation energy for the lowest barrier phosphate formation step is 14.7 kcal/mol. Unlike our previous studies of the CPA-catalyzed glycosylations, the covalent phosphate intermediate formation was not directly observed by low temperature ^{31}P, ^{13}C or ^{1}H NMR studies (*cf.* Scheme SI-S4). This is not surprising, however, as the computational studies indicate that covalent phosphate is 4.4 kcal/mol less stable than the reactant complex. Keeping in mind the low energy barrier for its formation and dissociation back, this step should be considered as being in equilibrium. During the reaction, the phosphate acetal would be formed only in trace quantities and exist as a steady-state intermediate, which could be observed in deuterium-exchange experiment with deuterium-labelled phosphoric acid (*cf.* SI-XVIII, Part C).

The second step of the phosphate-mediate pathway (Path C) has a reaction energy profile more consistent with a concerted S_Ni mechanism rather than an S_N1 mechanism, as no stable carbocation intermediates were detected (*cf.* Figure 2A). In this step the OH-group of 2,3-diol **4a** attacks the carbon atom of the methoxy cyclohexane fragment of the phosphate intermediate at the same time as the C-O phosphate bond cleaves. This second step is rate-limiting and shows the opposite regioselectivity compared to the concerted mechanism. That is, at both temperatures of interest the C3-protection was favored over the C2-protection ($\Delta\Delta G^{\ddagger}_{223}$ = 1.5 kcal/mol and $\Delta\Delta G^{\ddagger}_{273}$ = −1.6 kcal/mol, Table 6S-SI). Surprisingly, the activation energies of the rate-limiting step were also close to the ones computed for the concerted mechanism (Figure 2A).

The energy diagram summarizing our computational studies is provided in Figure 2A. Even though there was a slight preference for the phosphate mechanism, an obvious assignment of operating mechanism is not possible due to the energy difference being within the errors of the model. This situation, however, allows us to postulate that the concerted mechanism is preferred at low T, and the phosphate mechanism at high T. Invoking this switch in mechanism comes with a change in regioselectivity that nicely explains the experimental results depicted in Scheme 10. At low temperatures, the concerted mechanism (Path B) would therefore give rise to high C2-selectvity ($\Delta\Delta G^{\ddagger}$ (C2-C3) = −1.2 kcal/mol). At higher temperatures the phosphate mechanism (Path C) likely results in increased amounts of the C3 acetalization product ($\Delta\Delta G^{\ddagger}$ (C2-C3) = 1.5 kcal/mol).

Figure 1. Probing the reaction mechanism and stereochemistry of acetalization using deuterium-labeled d_3-1-methoxycyclohexene

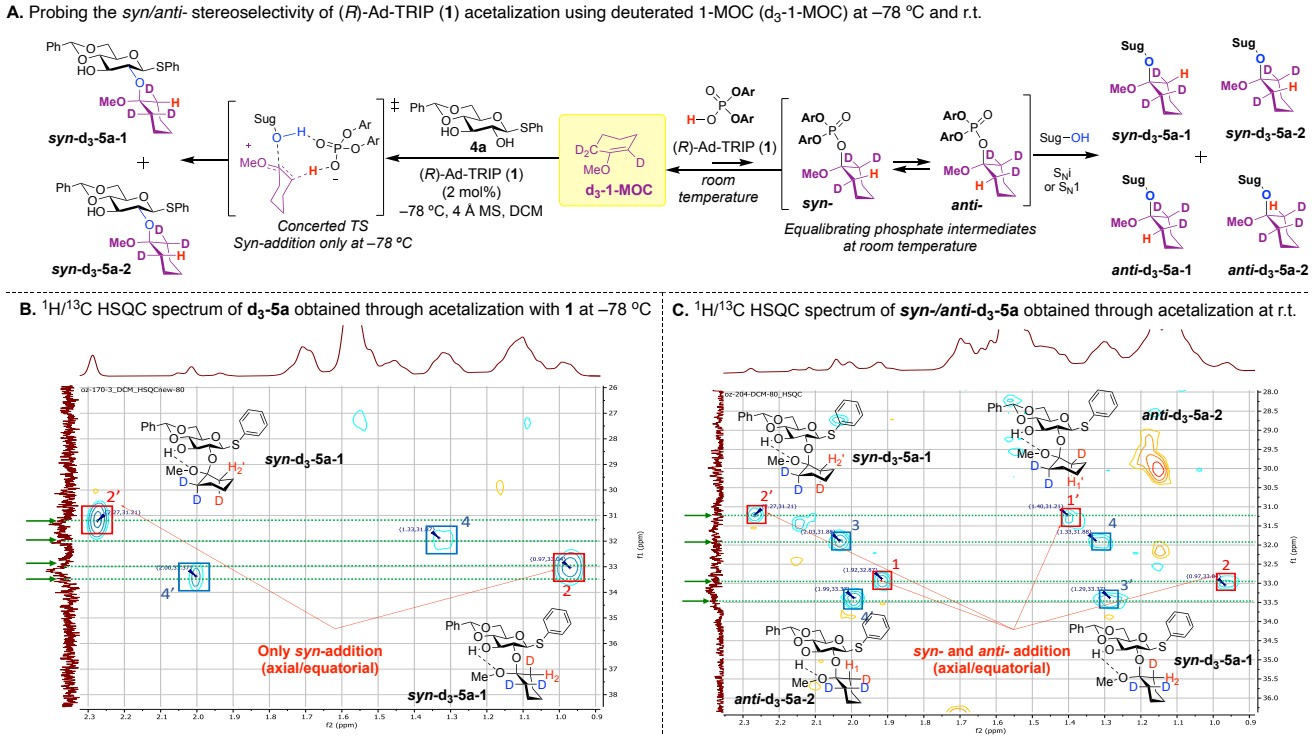

To experimentally probe our mechanistic hypothesis, a series of experiments with deuterium-labeled d_3-methoxycyclohenexe (d_3-MOC) was executed next (*cf.* Figure 1 and SI-XVIII, part D). Considering that our computational analysis (vide supra) suggested the concerted mechanism is operative

at –78°C, monosaccharide hydroxyl group and hydrogen addition to MOC double bond should be exclusively *syn*-specific. In contrast, the reaction proceeding through a phosphate intermediate should lead to both *syn*- and *anti*-addition of the hydroxyl group to the double bond due to fast equilibration though covalent phosphate. Using d_3-MOC as the electrophile, acetalization of **4a** was performed under the standard reaction conditions and resulted in the formation of deuterated acetals ***syn*-d$_3$-5a1** and ***syn*-d$_3$-5a2** (Figure 1A). The initial stereochemical assignment of ***syn*-d$_3$-5a** was hindered by the conformational flexibility of the MOC acetal moiety, which resulted in significant overlap of the MOC group signals. This coupled to the fact that two *syn*- and two *anti*- diastereomers might be formed by adding ROH to two different faces of MOC prompted us to carry additional NMR studies at –80°C. The NMR assignments were guided by computational analysis of the **d$_3$-5a** conformational space and their theoretically predicted ^{1}H and ^{13}C NMR shifts (cf. SI-X). The experiments at –80 ºC slowed the interconversion of the chair forms of ***syn*-d$_3$-5a1** and ***syn*-d$_3$-5a2**, and we observed four sets of ^{13}C signals present in the NMR spectrum of **d$_3$-5a**. Each of the diastereomeric *syn*-products ***syn*-d$_3$-5a1** and ***syn*-d$_3$-5a2** contributed a set of two conformers containing the MOC methoxy group in either an axial or an equatorial position in the cyclohexane ring (*cf.* Figure 1B, proton pairs 2-2' and 4-4'). The assignment of ^{1}H and ^{13}C NMR signals of ***syn*-d$_3$-5a1** and ***syn*-d$_3$-5a2** was carried using ^{1}H/^{13}C HSQC and EXCY-NOESY. This analysis was consistent with the calculated NMR shifts for the axial and equatorial conformers for these stereoisomers (*cf.* Scheme SI-X). Most importantly, significant magnetic anisotropy effects exhibited by the PhS-group on the top face of MOC are expected for the *syn*- rather than the *anti*-conformers, and that is indeed what is observed in low temperature NMR spectra of ***syn*-d$_3$-5a-1** and ***syn*-d$_3$-5a-2** (*cf.* Figure 1B and 1C).

To further validate this assignment, we independently synthesized and investigated a mixture of *syn*- and *anti*-diastereomers of **5a** (i.e. ***syn*-d$_3$-5a1**, ***syn*-d$_3$-5a2**, ***anti*-d$_3$-5a1** and ***anti*-d$_3$-5a1** by running acetalization with d_3-MOC at room temperature (*cf.* Figure 1A and 1C and Scheme X-SI). As expected, the mixture of ***syn*-d$_3$-5a1**, ***syn*-d$_3$-5a2**, ***anti*-d$_3$-5a1** and ***anti*-d$_3$-5a1** obtained by d_3-MOC acetalization at room temperature featured 8 HSQC cross peaks (*cf.* Figure 1C, proton pairs 1-1', 2-2', 3-3', 4-4') due to the additional equatorial and axial conformers for each of 4 diastereomers. These additional signals due to ***anti*-d$_3$-5a** isomers are consistent with the computed NMR data as well as the observed ^{1}H/^{13}C signals obtained for **5a** containing a nondeuterated MOC group. Altogether, these studies indicate that MOC protection at –78 ºC proceeds stereospecifically and results in *syn*- isomers while the same reaction results in the mixture of *syn*- and *anti*-isomers at room temperature. This is in good agreement with our other experimental and theoretical studies that predict a concerted asynchronous acetalization resulting in *syn*-product at –78 ºC. It is also consistent with the predictions that acetalization at higher temperature may proceeds through a competitive mechanism involving acetal phosphate-intermediate that is in equilibrium with (*R*)-Ad-TRIP (**1**) and 1-MOC at room temperature (*cf.* SI-X).

With the mechanistic picture in hand, transition state analysis was performed to identify the key structural features leading to different selectivities in each mechanism. The non-covalent interactions (NCIs) are known to be crucial in stabilizing or destabilizing the transition states when changes in energy by 1-2 kcal/mol can dramatically change the reaction selectivity. The graphical analysis[25] delineates NCI into three categories: blue, strong attraction; green, weak interaction; and red, strong repulsion. For the concerted mechanism(Figure 1B) there are two common regions of non-covalent interactions: (1) C-H van-der-Waals interactions of sugar backbone with catalyst adamantyl group and (2) enol ether C-H interaction with π-system of catalyst 3-aryl system. The most important interaction (3) is between the 4,6-benzalydine group and CPA isopropyl groups (circled for **TS$_2$**). The presence of such interaction can destabilize the transition state and make the C3-protection less favorable than the corresponding C2-pathway that lacks such steric repulsion (3). Remarkably, during the C2-protection via the phosphate-mediated mechanism, reactants and catalyst in **TS$_4$** are aligned almost in the same ways as for the concerted reaction (**TS$_1$**). There are some weak π···H-C interactions (4) that appear between the substrate **4a** and the MOC protecting group **PG**, but interactions (1) and (2) with the catalyst skeleton also are present. These similarities in NCI patterns for the **TS$_1$** and **TS$_4$** are in good agreement with almost identical TS energies for the C2-acetylization for both mechanisms. In contrast, the molecular alignment in **TS$_5$** (C3-protection) is significantly different from the concerted mechanism. The reactants are aligned in a more compact way and positioned further away from the catalytic pocket. The NCIs (1) and (2) arising from the 2,3-diol **4a**, MOC enol ether **PG** and the catalyst areminimized, and only interaction (4) between the reactants are clearly present. The absence of these NCIs in **TS$_5$** leads to its higher stability and, thus, the C3-protection prevails for the phosphate-mediated mechanism. Identified interactions and reactants alignment in catalytic cavity can be extrapolated and proved by looking at other substrates. First, using less bulky acetonide-protected compound **4m** gives only 12:1 regioselectivity favoring the C2-protected product. Two methyl groups in transition state **TS$_2$**-C3 should cause fewer destabilizing interactions with isopropyl groups reducing selectivity. Bulky C1-susbtituents in β-configuration (-SC$_6$H$_4$*t*Bu and -SNapth) shouldn't impact selectivity as they are positioned far away from catalyst and it is also in agreement with experimental data (substrates **4b** and **4d** also gives high 25:1 selectivity). Transition state **TS$_1$**-C2 reveals potential interactions of catalyst backbone with

Figure 2. Computational exploration of the reaction mechanism and stereochemical model for the regioselectivity

A. Energy diagram depicting potential reaction mechanisms at 223 K

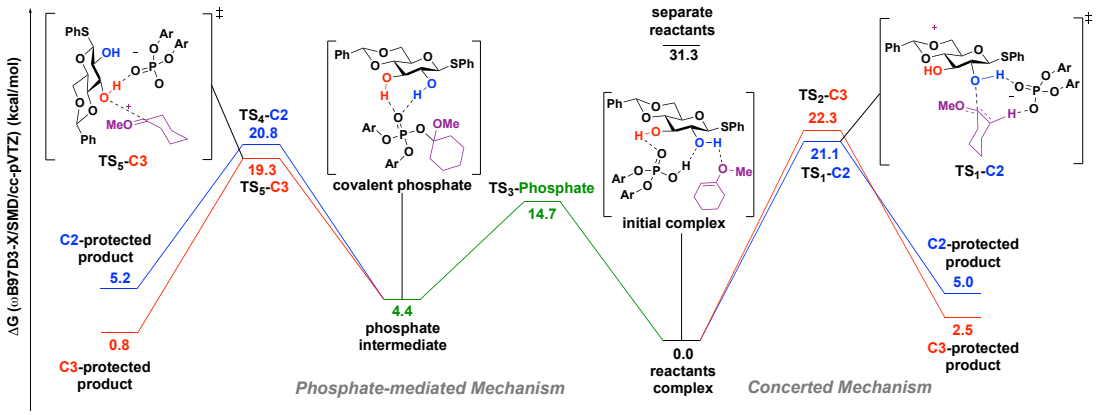

B. Noncovalent interaction analysis for regiocontrolling transition states TS_1 and TS_2 for concerted mechanism at 223 K

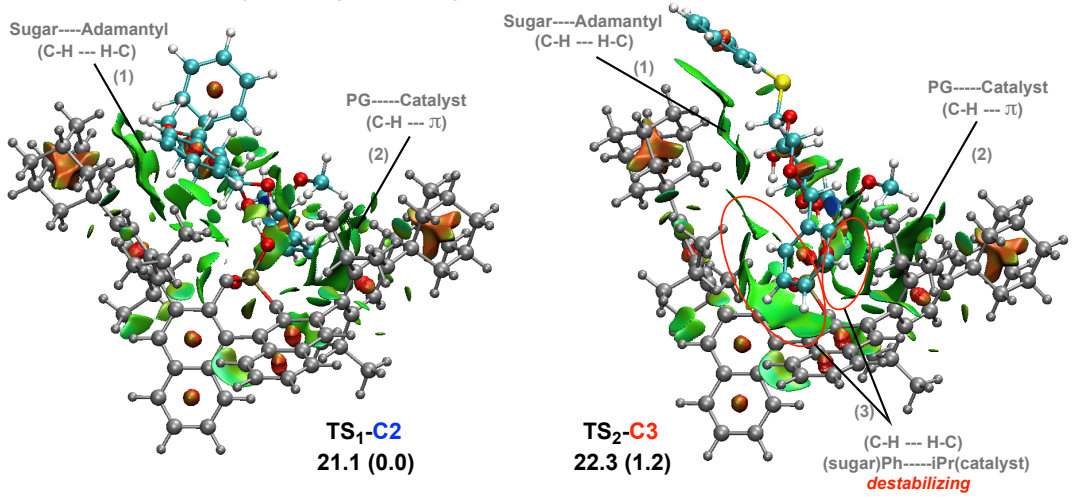

C. Noncovalent interaction analysis for regiocontrolling transition states TS_4 and TS_5 for phosphate-mediated mechanism at 223K

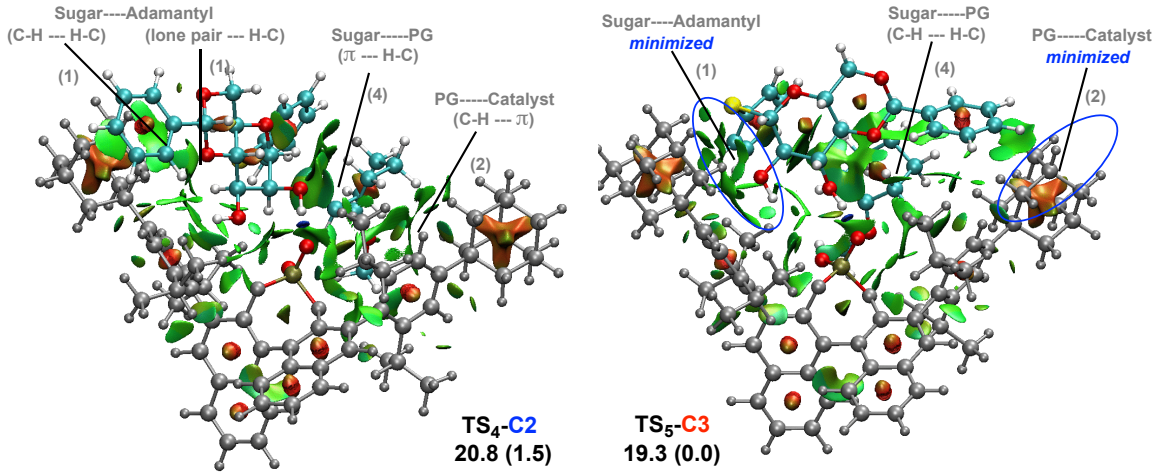

C1-susbtituent in α-configuration leading to its destabilization and to C3-selectivity as it was observed in case with *D*-glucose derivative **4f**.

In summary, the concerted asynchronous (Path B) and phosphate intermediate (Path C) mechanisms feature similar interactions in the transition states and molecular positions for the formation of the C2 isomer, which are reflected in negligible energy differences between these two pathways. Thus, the regioselectivity for the CPA-catalyzed acetal formation is determined by the steric interactions in the TS for the C3-protection. At low temperatures these results are consistent with the concerted mechanism being operative, where the sugar substrate alignment leading to the C3 product suffers from the interactions of 4,6-benzylidene acetal moiety with the catalyst. Considering the small difference in the RDS energy barriers for both pathways, the temperature can be an important factor in favoring one mechanism—and therefore one regioselectivity—over another.

3. CONCLUSION

In conclusion, this article describes the utility of regioselective acetalization reactions catalyzed by chiral phosphoric acids **1-3** for single-pot synthesis of 34 regioisomerically pure differentially functionalized mono- and disaccharide derivatives. To further improve the practicality of this approach, we developed two immobilized chiral phosphoric acids (*R*)-Ad TRIP (**2**) and (*S*)-SPINOL (**3**) that could be used to accomplish regiodivergent acetal protection of monosaccharide-based diols in good-to-excellent selectivities. Unlike their achiral counterparts, catalysts **2** and **3** allow to differentiate equatorial hydroxy groups and selectively produce regioisomeric products. In particular, (*R*)-Ad TRIP (**2**) demonstrated superior to monomeric **1** catalytic performance and selectivity, could be readily recycled by filtration and wash, and reused multiple times on 1.0 to 5.0 g scale acetalizations with loadings as low as 0.5 to 0.1 mol%. This enabled achieving significant catalyst economy, and regioselective one-pot gram scale syntheses of 6 differentially protected *D*-glucose derivatives **6a**, **6b**, **6f**, **6k**, **6p**, and **8e** were accomplished with the same 50 mg batch of catalyst **2**. The computational and mechanistic studies indicate complex temperature-dependent interplay of two reaction mechanisms. The dominant at low temperatures concerted asynchronous mechanism favors the formation of the C2 isomer due to destabilizing the TS leading to the C3 isomer interactions between the benzylidene acetal moiety of **4a** and catalyst **2**. This mechanism should lead to stereospecific addition of ROH resulting in *syn*-product, which is confirmed through the reaction of **4a** with deuterium labeled d_3-1-methoxycyclohexene (d_3-MOC). The developed stereochemical models allow expanding the scope of this transformation, and further studies focused on exploring more complex substrates and applying these transformations in continuous flow are the subjects of ongoing studies by our groups.

ASSOCIATED CONTENT

Supporting Information

Experimental procedures, ^{1}H and ^{13}C NMR spectra, and more detailed description of computational studies, are available free of charge via the Internet.

AUTHOR INFORMATION

Corresponding Authors

* nagorny@umich.edu, *paulzim@umich.edu

Author Contributions

§ S.W., O. Z. and J. L. are equally-contributing authors. All authors have given approval to the final version of the manuscript.

Funding Sources

PN and PZ thank NIH Common Fund grant U01GM125274 for supporting this work. PZ also thanks NIH grant R35-GM-128830, and PN also thanks R35 GM136341 for supporting the completion of this work.

Acknowledgement

We thank Prof. John Montgomery for the useful discussions during the preparation of this manuscript.

REFERENCES

(1) (a) Ernst, B; Magnani, J. L. "From carbohydrate leads to glycomimetic drugs" *Nature Rev. Drug Disc*. **2009**, *8*, 661; (b) Lepenies, B.; Seeberger, P. H. "The promise of glycomics, glycan arrays and carbohydrate-based vaccines" *Immunoph. Immunotoxic.* **2010**, *32*, 196.

(2) (a) C. S. Bennett "Principles of modern solid-phase oligosaccharide synthesis" *Org. Biomol. Chem*. **2014**, *12*, 1686; (b) Smoot, J. T.; Demchenko, A. V. "Oligosaccharide synthesis: from conventional methods to modern expeditious strategies" *Ad. Carbohydr. Chem. Biochem.* **2009**, *62*, 161; (c) Krasnova, L.; Wong, C.-H., "Oligosaccharide synthesis and translational innovation*" J. Am. Chem. Soc*. **2019**, *141*, 3735; (d) Seeberger, P. H.; Werz, D. B. "Synthesis and medical applications of oligosaccharides" *Nature* **2007**, *446*, 1046; (e) Seeberger, P. H.; Haase, W.-C. "Solid-phase oligosaccharide synthesis and combinatorial carbohydrate libraries" *Chem. Rev.* **2000**, *100*, 4349.

(3) (a) Filice, M.; Palomo, J. M. "Monosaccharide derivatives as central scaffolds in the synthesis of glycosylated drugs" *RSC Advances* **2012**, 2, 1729; (b) Wang, T.; Demchenko, A. V. "Synthesis of carbohydrate building blocks via regioselective uniform protection/deprotection strategies" *Org. Biomol. Chem.* **2019**, *17*, 4934; (c) Zulueta, M. M. L.; Janreddy, D.; Hung, S.-C. "One-pot methods for the protection and assembly of sugars*" Isr. J. Chem*. **2015**, *55*, 347.

(4) (a) Wang, C.-C.; Lee, J.-C.; Luo, S.-Y.; Kulkarni, S. S.; Huang, Y.-W.; Lee, C.-C.; Chang, K.-L.; Hung, S.-C. "Regioselective one-pot protection of carbohydrates" *Nature* **2007**, *446*, 896; (b) Wang, C.-C.; Kulkarni, S. S.; Lee, J.-C.; Luo, S.-Y.; Hung, S.-C. "Regioselective one-pot protection of glucose" *Nature Prot.* **2008**, *3*, 98; (c) Huang, T.-Y.;

Zulueta, M. M. L.; Hung, S.-C. "Regioselective one-pot protection, protection-glycosylation and protection-glycosylation-glycosylation of carbohydrates: a case study with D-glucose" *Org. Biomol. Chem.* **2014**, *12*, 376.
(5) (a) Francais, A.; Urban, D.; Beau, J.-M. "Tandem catalysis for a one-pot regioselective protection of carbohydrates: the example of glucose" *Angew. Chem. Int. Ed.* **2007**, *46*, 8662; (b) Beau, J.-M.; Bourdreux, Y.; Despras, G.; Gouasmat, A.; San Jose, G.; Urban, D.; Vauzeilles, B. "One-pot multistep regioselective protection of carbohydrates catalyzed by acids" *Protecting Groups: Strategies and Applications in Carbohydrate Chemistry*, First Edition, **2019**, Wiley-VCH Verlag GmbH & Co.
(6) (a) Giuliano, M. W.; Miller, S. J. "Site-selective reactions with peptide-based catalysts" *Top. Curr. Chem.* **2016**, *372*, 157; (b) Ueda, Y.; Kawabata, T. "Organocatalytic site-selective acylation of carbohydrates and polyol compounds" *Top. Curr. Chem.* **2016**, *372*, 303; (c) Lee, D.; Taylor, M. S. "Catalyst-controlled regioselective reactions of carbohydrate derivatives" *Synthesis* **2012**, *44*, 3421; (d) Lawandi, J.; Rocheleau, S.; Moitessier, N. "Regioselective acylation, alkylation, silylation and glycosylation of monosaccharides" *Tetrahedron* **2016**, *72*, 6283; (e) Dimakos, V.; Taylor, M. S. "Site-selective functionalization of hydroxyl groups in carbohydrate derivatives" *Chem. Rev.* **2018**, *118*, 11457; (f) Wang, T.; Demchenko, A. V. "Synthesis of carbohydrate building blocks via regioselective uniform protection/deprotection strategies" *Org. Biomol. Chem*. **2019**, *17*, 4934.
(7) Selected examples of site-selective achiral catalyst promoted protection of sugars: (a) Dimakos, V.; Garrett, G. E.; Taylor, M. S. "Site-selective, copper-mediated O-arylation of carbohydrate derivatives" *J. Am. Chem. Soc*. **2017**, *139*, 15515; (b) Lee, D.; Taylor, M. S. "Borinic acid-catalyzed regioselective acylation of carbohydrate derivatives" *J. Am. Chem. Soc*. **2011**, *133*, 3724; (c) Wu, J.; Li, X.; Qi, X.; Duan, X.; Cracraft, W. L.; Guzei, I. A.; Liu, P.; Tang, W. "Site-selective and stereoselective O-alkylation of glycosides by Rh(II)-catalyzed carbenoid insertion" *J. Am. Chem. Soc*. **2019,** *141*, 19902; (d) Peng, P.; Linseis, M.; Winter, R. F.; Schmidt, R. R. "Regioselective acylation of diols and triols: the cyanide effect" *J. Am. Chem. Soc.* **2016**, *138*, 6002; (e) Li, T.; Li, T.; Linseis, M.; Wang, F.; Winter, R. F.; Schmidt, R. R.; Peng, P. "Catalytic regioselective benzoylation of 1,2-trans-diols in carbohydrates with benzoyl cyanide: the axial oxy group effect and the action of achiral and chiral amine catalysts" *ACS Catalysis* **2020**, *10*, 11406; (f) Huber, F.; Kirsch, S. F. "Site-selective acylations with tailor-made catalysts" *Chem.-Eur. J.* **2016**, *22*, 5914.
(8) (a) Sculimbrene, B. R.; Miller, S. J. "Discovery of a catalytic asymmetric phosphorylation through selection of a minimal kinase mimic: a concise total synthesis of D-myo-inositol-1-phosphate" *J. Am. Chem. Soc.* **2001**, *123*, 10125; (b) Sculimbrene, B. R.; Morgan, A. J.; Miller, S. J. "Enatniodivergence in small-molecule catalysis of asymmetric phosphorylation: concise total syntheses of the enantiomeric D-myo-inositol-1-phosphate and D-myo-inositol-3-phosphate" *J. Am. Chem. Soc.* **2002**, *124*, 11653; (c) Griswold, K. S.; Miller, S. J. "A peptide-based catalyst approach to regioselective functionalization of carbohydrates" *Tetrahedron* **2003**, *59*, 8869; (d) Allen, C. L.; Miller, S. "Chiral copper(II) complex-catalyzed reactions of partially protected carbohydrates" J. *Org. Lett.* **2013**, *15*, 6178.
(9) (a) Kawabata, T.; Muramatsu, W.; Nishio, T.; Shibata, T.; Schedel, H. "A catalytic one-step process for the chemo- and regioselective acylation of monosaccharides" *J. Am. Chem. Soc.* **2007**, *129*, 12890; (b) Muramatsu, W.; Mishiro, K.; Ueda, Y.; Furuta, T.; Kawabata, T. "Perfectly regioselective and sequential protection of glucopyranosides" *Eur. J. Org. Chem.* **2010**, *5*, 827.
(10) (a) Xiao, G.; Cintron-Rosado, G. A.; Glazier, D. A.; Xi, B.; Liu, C.; Tang, W. "Catalytic site-selective acylation of carbohydrates directed by cation-n interactions" *J. Am. Chem. Soc*. **2017**, *139*, 4346; (b) Blaszczyk, S. A.; Xiao, G.; Wen, P.; Hao, H.; Wu, J.; Wang, B.; Carattino, F.; Li, Z.; Glazier, D. A.; McCarty, B. J.; Liu, P.; Tang, W. "S-adamantyl group directed site-selective acylation and its applications in the streamlined assembly of oligosaccharides" *Angew. Chem. Int. Ed.* **2019**, *58,* 9542.
(11) Selected publications on chiral catalyst-controlled functionalization of carbohydrates: (a) Li, R.-Z.; Tang, H.; Wan, L.; Zhang, X.; Fu, Z.; Liu, J.; Yang, S.; Jia, D.; Niu, D. "Site-divergent delivery of terminal propargyls to carbohydrates by synergistic catalysis" *Chem* **2017**, *3*, 834; (b) Sun, X.; Lee, H.; Lee, S.; Tan, K. L. "Catalyst recognition of cis-1,2-diols enables site-selective functionalization of complex molecules" *Nature Chem.* **2013**, *5*, 790; (c) Shang, W.; Mou, Z.-D.; Tang, H.; Zhang, X.; Liu, J.; Fu, Z.; Niu, D. "Site-selective O-arylation of glycosides" *Angew. Chem. Int. Ed*. **2018**, *57*, 314; (d) Hu, G.; Vasella, A. "Regioselective benzoylation of 6-O-protected and 4,6-O-diprotected hexopyranosides as promoted by chiral and achiral ditertiary 1,2-diamines" *Helv. Chim. Acta* **2002**, *85*, 4369.
(12) (a) Lee, J.; Borovika, A.; Khomutnyk, Y.; Nagorny, P. " Chiral phosphoric acid-catalyzed desymmetrizative glycosylation of 2-deoxystreptamine and its application to aminoglycoside synthesis" *Chem. Commun*. **2017**, *53*, 8976; b) Tay, J.-H.; Arguelles, A. J.; DeMars II, M. D.; Zimmerman, P. M.; Sherman, D. H.; Nagorny, P." Chiral Phosphoric Acid-controlled Regioselective Glycosylation of 12-membered Macrolides" *J. Am. Chem. Soc*. **2017**, *139*, 8570; c) Khomutnyk, Y. Y.; Arguelles, A. J.; Winschel, G. A.; Sun, Z.; Zimmerman, P. M.; Nagorny, P. " Studies of the Mechanism and Origins of Enantioselectivity for the Chiral Phosphoric Acid-Catalyzed Stereoselective Spiroketalization" *J. Am. Chem. Soc.* **2016**, *138*, 144; d) e) Nagorny, P.; Sun, Z.; Winschel, G. A. "Chiral Phosphoric Acid Catalyzed Stereoselective spiroketalizations" *Synlett* **2013**, *24*, 661; f) Sun, Z.; Winschel, G. A.; Borovika, A.; Nagorny, P. "Chiral Phosphoric Acid-Catalyzed Enantioselective and Diastereoselective Spiroketalizations Chiral Phosphoric Acid-Catalyzed Enantioselective and Diastereoselective Spiroketalizations" *J. Am. Chem. Soc.* **2012**, *134*, 8074.
(13) Mensah, E.; Camasso, N.; Kaplan, W.; Nagorny, P. " Chiral Phosphoric Acid-Directed Regioselective Acetalization of Carbohydrate-Derived 1,2-diols" *Angew. Chem. Int. Ed.* **2013**, *52*, 13939.
(14) Selected examples of CPA-catalyzed stereoselective formation and cleavage of acetal protecting groups: (a) Kim, J. H.; Coric, I.; Palumbo, C.; List, B. "Resolution of diols via catalytic asymmetric acetalization" *J. Am. Chem. Soc.* **2015**, *137*, 1778; (b) Yamanaka, T.; Kondoh, A.; Terada, M. "Kinetic resolution of racemic amino alcohols through intermolecular acetalization catalyzed by a chiral Bronsted acid" *J. Am. Chem. Soc*. **2015**, *137*, 1048; (c) Ye, B.; Zhao, J.; Zhao, K.; McKenna, J. M.; Toste, D. F. "Chiral diaryliodonium phosphate enables light driven diastereoselective a-C(sp3)-H acetalization" *J. Am. Chem. Soc.* **2018**, *140*, 8350; (d) Meng, S.-S.; Liang, Y.; Cao, K.-S.; Zou, L.; Lin, X.-B.; Yang, H.; Houk, K. N.; Zheng, W.-H. "Chiral phosphoric acid catalyzed highly enantioselective desymmetrization of 2-substituted and 2,2-disubstituted 1,3-diols via oxidative cleavage of benzylidene acetals" *J. Am. Chem. Soc*. **2014**, *136*, 12249; (e) Hyudo, K.; Gandhi, S.; van Gemmeren, M.; List, B. "Bronsted acid catalyzed asymmetric silylation of alcohols" *Synlett* **2015**, *26*, 1093; (f) Kimura, T.; Sekine, M.; Takahashi, D.; Toshima, K. "Chiral Bronsted acid mediated glycosylation with recognition of alcohol chirality" *Angew. Chem. Int. Ed*. **2013**, *52*, 12131.

(15) (a) Akiyama, T.; Itoh, J.; Yokota, K.; Fuchibe, K. "Enantioselective Mannich-type reaction catalyzed by a chiral Bronsted acid" *Angew. Chem. Int. Ed.* **2004**, *43*, 1566; (b) Uraguchi, D.; Terada, M. "Chiral Bronsted acid-catalyzed direct Mannich reactions via electrophilic activation" *J. Am. Chem. Soc.* **2004**, *126*, 5356.
(16) Hayashi, Y. "Pot economy and one-pot synthesis" *Chem. Science* **2016**, *7*, 866.
(17) (a) Wuts, P. G. M.; Greene, T. W. *Green's Protective Groups in Organic Synthesis,* 4th ed.; John Wiley & Sons, Inc.; Hoboken, NJ. **2007**, pp 59-79; b) Kocienski, P. J. *Protecting Groups*, 3d ed.; Georg Thieme Verlag; Stuttgart **2005**, pp 315-320.
(18) (a) Benaglia, M.; Puglisi, A.; Cozzi, F. "Polymer-supported organic catalysts" *Chem. Rev.* **2003**, *103*, 3401; (b) Kristensen, T. E.; Hansen, T. "Polymer-supported chiral organocatalysts: synthetic strategies for the road towards affordable polymeric immobilization" *Eur. J. Org. Chem.* **2010**, *17*, 3179; (c) Rodriguez-Escrich, C.; Pericas, M. A. "Organocatalysis on tap: enantioselective continuous flow processes mediated by solid-supported chiral organocatalysts" *Eur. J. Org. Chem.* **2015**, *6*, 1173; (d) Rodriguez-Escrich, C.; Pericas, M. A. "Catalytic enantioselective flow processes with solid-supported chiral catalysts" *Chem. Rec.* ***2019****, 19,* 1872.
(19) (a) Bartoszek, M.; Beller, M.; Deutsch, J.; Klawonn, M.; Kockritz, A.; Nemati, N.; Pews-Davtyan, A. "A convenient protocol for the synthesis of axially chiral Brønsted acids" *Tetrahedron* **2008**, *64*, 1316; (b) Rueping, M.; Sugiono, E.; Steck, A.; Theissmann, T. "Synthesis and application of polymer-supported chiral Brønsted acid organocatalysts" *Adv. Synth. Catal.* **2010**, *352*, 281; (c) Bleschke, C.; Schmidt, J.; Kundu, D. S.; Blechert, S.; Thomas, A. "A chiral microporous polymer network as asymmetric heterogeneous organocatalyst" *Adv. Synth. Catal*. **2011**, *353*, 3101; (d) Kundu, D. S.; Schmidt, J.; Bleschke, C.; Thomas, A.; Blechert, S. "A microporous BINOL-derived phosphoric acid" *Angew. Chem. Int. Ed.* **2012**, *51*, 5456; (e) Osorio-Planes, L.; Rodriguez-Escrih, C.; Pericas, M. A. "Enantioselective continuous-flow production of 3-indolylmethanamines mediated by an immobilized phosphoric acid catalyst" *Chem. Eur. J.* **2014**, *20*, 2367.
(20) (a) Clot-Almenara, L.; Rodriguez-Escrich, C.; Osorio-Planes, L.; Pericas, M. A. "Polystyrene-supported TRIP: a highly recyclable catalyst for batch and flow enantioselective allylation of aldehydes" *ACS Catal.* **2016**, *6*, 7642; (b) Lai, J.; Fianchini, M.; Pericas, M. A. "Development of immobilized SPINOL-derived chiral phosphoric acids for catalytic continuous flow processes. Use in the catalytic desymmetrization of 3,3-disubstituted oxetanes" *ACS Catal.* **2020**, *10*, 14971.
(21) (a) Kanomata, K.; Toda, Y.; Shibata, Y.; Yamanaka, M.; Tsuzuki, S.; Gridnev, I. D.; Terada, M. "Secondary stereocontrolling interactions in chiral Bronsted acid catalysis: study of a Petasis-Ferrier-type rearrangement catalyzed by chiral phosphoric acids" *Chem. Sci.* **2014**, *5*, 3515; (b) Maskeri, M. A.; Brueckner, A. C.; Feoktistova, T.; O'Connor, M. J.; Walden, D. M.; Cheong, P. H.-Y.; Scheidt, K. A. "Mechanism and origins of selectivity in the enantioselective *oxa*-Picter-Spengler reaction: A cooperative catalytic complex from a hydrogen bond donor and chiral phosphoric acid" *Chem. Sci.* **2020**, *11*, 8736; (c) Lee, S.; Kaib, P. S. J.; List, B. "Asymmetric catalysis via cyclic, aliphatic oxocarbenium ion" *J. Am. Chem. Soc*. **2017**, *139,* 2156; (d) Das, S.; Liu, L.; Zheng, Y.; Alachraf, M. W.; Thiel, W.; De, C. K.; List, B. "Nitrated confined imidodiphosphates enable a catalytic asymmetric oxa-Pictet-Spengler reaction" *J. Am. Chem. Soc.* **2016**, *138,* 9429.
(22) Sun, Z.; Winschel, G. A.; Zimmerman, P. M.; Nagorny, P. "Enantioselective synthesis of piperidines through the formation of mixed chiral phosphoric acid acetals: experimental and theoretical studies" *Angew. Chem. Int. Ed.* **2014***, 53,* 11194.
(23) Zimmerman, P. "Reliable Transition State Searches Integrated with the Growing String Method" *J. Chem. Theory Comput.* **2013**, *9*, 3043.
(24) Zimmerman, P. M. "Single-Ended Transition State Finding with the Growing String Method" J. Comput. Chem. 2015, 36, 601.
(25) Contreras-garcía, J.; Johnson, E. R.; Keinan, S.; Chaudret, R.; Piquemal, J.; Beratan, D. N.; Yang, W. "NCIPLOT: A Program for Plotting Noncovalent Interaction Regions" *J. Chem. Theory Comput.* **2011**, *7*, 625.